

# DSN Baseline Coordinate and Station Location Errors Induced by Earth Orientation Errors

S. W. Thurman  
Navigation Systems Section

*Earth orientation errors, consisting of errors in knowledge of the Earth's polar axis motion and rotation period, introduce systematic errors into the radio metric data that are acquired by the Deep Space Network (DSN) and used for spacecraft navigation. This article contains a brief analysis of the sensitivity of station location and baseline coordinates to Earth orientation errors, and of the uncertainties induced in DSN station location and intercontinental baseline coordinates by current levels of Earth orientation uncertainty. The analysis indicates that while the sensitivities of certain DSN baseline coordinates differ by more than an order of magnitude, DSN station locations and baseline coordinates in general have Earth orientation error sensitivities of similar magnitudes. Typical (not maximum) DSN station location uncertainties were found to be 6 to 8 cm in spin-radius and z-height coordinates, and approximately 40 nrad in station longitudes. Baseline coordinate uncertainties ranged from 1 to 13 cm in spin-radius and z-height, with longitude uncertainties of about the same (40 nrad) magnitude as those of the individual stations.*

## I. Introduction

The advent of radio interferometry in spacecraft navigation, in the form of data types based on Very Long Baseline Interferometry (VLBI) such as Delta-Differenced One-Way Range ( $\Delta$ DOR), and quasi-VLBI data types such as differenced Doppler and range, has brought about great increases in navigation accuracy over the past ten years. Interferometric data types, especially differenced Doppler and range, can all be very sensitive to errors in baseline length and orientation. Even if the coordinates of a given baseline are known perfectly in an Earth-fixed reference frame, imperfect knowledge of the orientation of the Earth-fixed frame, with respect to the inertial reference frame that is being used for navigation computations, will intro-

duce systematic errors into the baseline coordinate values used in processing the data. The sensitivities of the two intercontinental baselines used by the DSN for acquiring VLBI and quasi-VLBI data types are of particular interest. These baselines are formed between DSN stations in Madrid and Goldstone, and Canberra and Goldstone, respectively.

The analysis presented below establishes the sensitivities of the baselines formed by Deep Space Stations (DSSs) 43 and 14, which will hereinafter be referred to as the Canberra-Goldstone baseline, and DSSs 63 and 14, which will hereinafter be referred to as the Madrid-Goldstone baseline, to Earth orientation errors, a phrase that refers

collectively to errors in knowledge of the Earth's polar motion and rotation period. In addition, the sensitivities of each of the three individual stations are also given, since the conventional Doppler and range data acquired by these and other stations are also affected by station location errors induced through Earth orientation errors. Since the antennas at each of the three DSN complexes are located very close to one another (only a few kilometers apart in most cases), the Earth orientation error sensitivities computed for DSSs 14, 43, and 63 are nearly identical to those of the other antennas located at the same complexes.

## II. Analysis

The location of a tracking station in an Earth-centered inertial reference frame is depicted in Fig. 1. The Earth-centered inertial reference frame will be taken here to be the Earth mean equator and equinox of J2000.0, although the analysis would be equally valid for any other Earth-centered inertial frame that is referred to the Earth's equator (e.g., the Earth mean equator and equinox of B1950.0). The three coordinates used to describe Earth orientation error are also shown in Fig. 1 and are defined as follows:  $X$  is a small shift in the Earth's north pole toward the equator along the Greenwich meridian,  $Y$  is a small shift in the Earth's north pole in a direction 90 deg west of Greenwich, and  $UT$  is a small rotation about the Earth's spin axis to the east. These rotations do not change the actual locations of tracking stations; they introduce errors into the coordinate transformation used to compute the station locations in an Earth-centered inertial reference frame. In this article,  $X$  and  $Y$  are expressed in centimeters, while  $UT$  is expressed in milliseconds. The actual determination of station locations in inertial space also requires knowledge of the precession and nutation of the Earth's nominal axis of rotation. These motions, however, are mostly periodic and do not require regular monitoring and calibration, as do the Earth's polar motion ( $X$ ,  $Y$ ) and rotation period ( $UT$ ), which can vary rapidly with time. (The Earth's rotation period has been observed in extreme cases to change by up to 1 msec over periods of 1 to 3 days; polar motion generally varies more slowly than this, and more predictably as well.) Only Earth orientation errors will be addressed explicitly in this article.

The partial derivatives of the cylindrical station coordinates  $r$ ,  $z$ , and  $\lambda$  with respect to  $X$ ,  $Y$ , and  $UT$  have been derived previously.<sup>1</sup> They are

$$\begin{aligned}\partial r/\partial(X, Y, UT) &= \left(\frac{z}{R_p}\right) [-\cos \lambda, \sin \lambda, 0] \\ \partial z/\partial(X, Y, UT) &= \left(\frac{r}{R_p}\right) [\cos \lambda, -\sin \lambda, 0] \\ \partial \lambda/\partial(X, Y, UT) &= \left(\frac{1}{R_p}\right) [(z/r) \sin \lambda, (z/r) \cos \lambda, R_p \omega]\end{aligned}\quad (1)$$

In Eq. (1),  $R_p$  is the Earth's polar radius and  $\omega$  is the Earth's rotation rate. The vector components of the baseline between two stations can also be expressed in terms of cylindrical coordinates.

Using the Earth-centered inertial reference system shown in Fig. 1, the baseline vector  $\vec{B}$  between two stations can be written as a function of the cylindrical baseline coordinates  $r_B$ ,  $z_B$ , and  $\lambda_B$  as

$$\vec{B} = \vec{r}_{s_1} - \vec{r}_{s_2} = [r_B \cos(\alpha_g + \lambda_B), r_B \sin(\alpha_g + \lambda_B), z_B] \quad (2)$$

where

$$\begin{aligned}\vec{r}_{s_1} &= [r_1 \cos(\alpha_g + \lambda_1), r_1 \sin(\alpha_g + \lambda_1), z_1] \\ \vec{r}_{s_2} &= [r_2 \cos(\alpha_g + \lambda_2), r_2 \sin(\alpha_g + \lambda_2), z_2]\end{aligned}\quad (3)$$

In Eq. (2),  $\alpha_g$  is the right ascension of the Greenwich meridian. The cylindrical baseline coordinates are themselves functions of the cylindrical coordinates of the two stations comprising the baseline

$$\begin{aligned}r_B &= [r_1^2 + r_2^2 - 2r_1 r_2 \cos(\lambda_1 - \lambda_2)]^{1/2} \\ z_B &= z_1 - z_2 \\ \lambda_B &= \tan^{-1} [(r_1 \sin \lambda_1 - r_2 \sin \lambda_2)/(r_1 \cos \lambda_1 - r_2 \cos \lambda_2)]\end{aligned}\quad (4)$$

The partial derivatives of the baseline coordinates with respect to  $X$ ,  $Y$ , and  $UT$  are obtained simply by taking the partial derivatives of Eq. (4) with respect to the two sets

<sup>1</sup> R. K. Russell, "Computation of Polar Motion and Universal Time Partial Derivatives," JPL Engineering Memorandum 391-270 (internal document), Jet Propulsion Laboratory, Pasadena, California, January 14, 1972.

of station coordinates, and then using the station partial derivatives given in Eq. (1) to form the desired result

$$\partial r_B / \partial X = \frac{\partial r_B}{\partial r_1} \frac{\partial r_1}{\partial X} + \frac{\partial r_B}{\partial r_2} \frac{\partial r_2}{\partial X} + \frac{\partial r_B}{\partial \lambda_1} \frac{\partial \lambda_1}{\partial X} + \frac{\partial r_B}{\partial \lambda_2} \frac{\partial \lambda_2}{\partial X}$$

$$\partial r_B / \partial Y = \frac{\partial r_B}{\partial r_1} \frac{\partial r_1}{\partial Y} + \frac{\partial r_B}{\partial r_2} \frac{\partial r_2}{\partial Y} + \frac{\partial r_B}{\partial \lambda_1} \frac{\partial \lambda_1}{\partial Y} + \frac{\partial r_B}{\partial \lambda_2} \frac{\partial \lambda_2}{\partial Y}$$

$$\partial r_B / \partial UT = \frac{\partial r_B}{\partial \lambda_1} \frac{\partial \lambda_1}{\partial UT} + \frac{\partial r_B}{\partial \lambda_2} \frac{\partial \lambda_2}{\partial UT} \quad (5)$$

$$\partial \lambda_B / \partial X = \frac{\partial \lambda_B}{\partial r_1} \frac{\partial r_1}{\partial X} + \frac{\partial \lambda_B}{\partial r_2} \frac{\partial r_2}{\partial X} + \frac{\partial \lambda_B}{\partial \lambda_1} \frac{\partial \lambda_1}{\partial X} + \frac{\partial \lambda_B}{\partial \lambda_2} \frac{\partial \lambda_2}{\partial X}$$

$$\partial \lambda_B / \partial Y = \frac{\partial \lambda_B}{\partial r_1} \frac{\partial r_1}{\partial Y} + \frac{\partial \lambda_B}{\partial r_2} \frac{\partial r_2}{\partial Y} + \frac{\partial \lambda_B}{\partial \lambda_1} \frac{\partial \lambda_1}{\partial Y} + \frac{\partial \lambda_B}{\partial \lambda_2} \frac{\partial \lambda_2}{\partial Y}$$

$$\partial \lambda_B / \partial UT = \frac{\partial \lambda_B}{\partial \lambda_1} \frac{\partial \lambda_1}{\partial UT} + \frac{\partial \lambda_B}{\partial \lambda_2} \frac{\partial \lambda_2}{\partial UT} \quad (6)$$

$$\partial z_B / \partial X = \frac{\partial z_B}{\partial z_1} \frac{\partial z_1}{\partial X} + \frac{\partial z_B}{\partial z_2} \frac{\partial z_2}{\partial X}$$

$$\partial z_B / \partial Y = \frac{\partial z_B}{\partial z_1} \frac{\partial z_1}{\partial Y} + \frac{\partial z_B}{\partial z_2} \frac{\partial z_2}{\partial Y}$$

$$\partial z_B / \partial UT = 0 \quad (7)$$

The partial derivatives of the baseline coordinates, given in Eq. (4), with respect to the station coordinates, are

$$\begin{aligned} \partial r_B / \partial (r_1, z_1, \lambda_1) &= (1/r_B) [r_1 - r_2 \cos(\lambda_1 - \lambda_2), 0, r_1 r_2 \sin(\lambda_1 - \lambda_2)] \\ \partial r_B / \partial (r_2, z_2, \lambda_2) &= (1/r_B) [r_2 - r_1 \cos(\lambda_1 - \lambda_2), 0, -r_1 r_2 \sin(\lambda_1 - \lambda_2)] \end{aligned} \quad (8)$$

$$\begin{aligned} \partial \lambda_B / \partial (r_1, z_1, \lambda_1) &= \frac{\cos^2 \lambda_B}{(r_1 \cos \lambda_1 - r_2 \cos \lambda_2)^2} \\ &\times \begin{bmatrix} -r_2 \sin(\lambda_1 - \lambda_2) \\ 0 \\ r_1^2 - r_1 r_2 \cos(\lambda_1 - \lambda_2) \end{bmatrix}^T \\ \partial \lambda_B / \partial (r_2, z_2, \lambda_2) &= \frac{\cos^2 \lambda_B}{(r_1 \cos \lambda_1 - r_2 \cos \lambda_2)^2} \\ &\times \begin{bmatrix} r_1 \sin(\lambda_1 - \lambda_2) \\ 0 \\ r_2^2 - r_1 r_2 \cos(\lambda_1 - \lambda_2) \end{bmatrix}^T \end{aligned} \quad (9)$$

$$\partial z_B / \partial (r_1, z_1, \lambda_1) = [0, 1, 0]$$

$$\partial z_B / \partial (r_2, z_2, \lambda_2) = [0, -1, 0] \quad (10)$$

The partial derivatives in Eqs. (5) through (7) represent the sensitivities of a set of baseline coordinates to Earth orientation errors. It has been shown that the expressions in Eqs. (5) through (7), when combined with Eqs. (8) through (10), can be reduced to a form that is identical to the sensitivities given in Eq. (1) for the individual stations, with the understanding that the spin-radius ( $r$ ),  $z$ -height ( $z$ ), and longitude ( $\lambda$ ) in Eq. (1) refer to baseline coordinates instead of station coordinates.<sup>2</sup> Using Eq. (1), the sensitivities of DSS 14 (Goldstone), DSS 43 (Canberra), and DSS 63 (Madrid) with respect to errors in  $X$ ,  $Y$ , and  $UT$  were computed, and are given in Table 1. Using Eqs. (8) through (10) and the station location sensitivities from Table 1, sensitivity values were computed for the Canberra-Goldstone (DSS 43-DSS 14) and Madrid-Goldstone (DSS 63-DSS 14) baselines and are given in Table 2. The station locations and baseline coordinates used in these calculations were those determined by Moyer<sup>3</sup> and are given in Table 5. The station longitudes given in Table 5 are the angle of rotation in an easterly direction from the Greenwich meridian to the station meridian. Using the station and baseline Earth orientation partial derivatives from Tables 1 and 2, station location and

<sup>2</sup> This equivalence has been demonstrated by W. M. Folkner, Tracking Systems and Applications, Section 335, Jet Propulsion Laboratory, Pasadena, California.

<sup>3</sup> T. D. Moyer, "Station Location Sets Referred to the Radio Frame," JPL Interoffice Memorandum 314.5-1334 (internal document), Jet Propulsion Laboratory, Pasadena, California, February 24, 1989.

baseline coordinate uncertainties ( $1\sigma$ ) were computed for representative levels of uncertainty in  $X$ ,  $Y$ , and  $UT$ , assuming that the errors in these parameters are statistically independent. The uncertainties ( $1\sigma$ ) assumed for  $X$  and  $Y$  were 10 cm, while 0.5 msec was assumed for  $UT$ . These figures are typical (not maximum) uncertainty levels for Earth orientation angles predicted one week ahead, which are derived using calibration data obtained from the DSN's Timing and Earth Motion Precision Observations (TEMPO) service. TEMPO Earth orientation predictions are derived from weekly VLBI observations of extragalactic radio sources.<sup>4</sup> Table 3 contains the DSN station location uncertainties induced by these Earth orientation uncertainties, and Table 4 contains the corresponding baseline uncertainties.

### III. Discussion

Generally speaking, Earth orientation errors, as seen in Tables 3 and 4, affect DSN station locations and intercontinental baselines fairly equally, with the significant exception of the Madrid-Goldstone baseline's  $r_B$  coordinate (spin radius), which is over an order of magnitude less sensitive to  $X$  and  $Y$  errors than the spin radius of the Canberra-Goldstone baseline. Also note that only baseline longitudes are affected by  $UT$  errors. In fact, the baseline longitudes are dominated by  $UT$  errors; improvements in  $X$  and  $Y$  accuracies will have very little impact on baseline longitude accuracies until  $UT$  calibration

accuracy is improved. Studies of the information content of Doppler data, and DSN X-band (8.4-GHz) Doppler data in particular, have indicated that Doppler is very sensitive to station spin-radius and longitude errors [1], and that spin-radius accuracies of 10 cm or better and longitude accuracies of about 30 nrad are needed in order to prevent station location errors from being the largest contributor to total navigation-error uncertainty when using Doppler data [2]. As can be seen in Table 3, though, present levels of Earth orientation uncertainty alone induce near-10-cm uncertainties in spin-radius values, and 38-nrad uncertainties in station longitudes.

Differenced range and Doppler data types, which have the potential to deliver medium-accuracy (50 to 100 nrad) angular measurements for deep-space navigation, may be very sensitive to baseline coordinate errors [3,4]. With differenced Doppler data, spacecraft declination is estimated by measuring the amplitude of the sinusoidal data signature, which is a function of both declination and the baseline spin radius; declination is determined from single-station Doppler data in the same manner, except that the spin radius in this case is that of the station itself. Since differenced Doppler's ability to determine spacecraft angular coordinates is superior to that of single-station Doppler, X-band differenced Doppler will require baseline coordinate accuracies even greater than the station location accuracies needed for single-station X-band Doppler. Generally speaking, it appears that Earth orientation error uncertainties will have to be reduced substantially from their current levels before the full potential of high-accuracy differenced data types can be effectively utilized.

---

<sup>4</sup>H. N. Royden, "TSAC (Tracking System Analytic Calibrations) Overview," JPL RTOP 63 Seminar Presentation, Jet Propulsion Laboratory, Pasadena, California, July 12, 1988.

## Acknowledgments

The author thanks Jim Ulvestad, Bill Folkner, and Alan Steppe for their comments and suggestions on earlier drafts of this article.

## References

- [1] T. W. Hamilton and W. G. Melbourne, "Information Content of a Single Pass of Doppler Data from a Distant Spacecraft," *JPL Space Programs Summary 37-39*, vol. 3, Jet Propulsion Laboratory, Pasadena, California, pp. 18–23, March–April 1966.
- [2] S. W. Thurman, "Comparison of Earth-Based Radio Metric Data Strategies for Deep Space Navigation," Paper AIAA-90-2908, AIAA/AAS Astrodynamics Conference, Portland, Oregon, August 20–22, 1990.
- [3] S. W. Thurman, "Deep-Space Navigation With Differenced Data Types, Part I: Differenced Range Information Content," *TDA Progress Report 42-103* (this issue), vol. July–September 1990, Jet Propulsion Laboratory, Pasadena, California, pp. 47–60, November 15, 1990.
- [4] S. W. Thurman, "Deep-Space Navigation With Differenced Data Types, Part II: Differenced Doppler Information Content," *TDA Progress Report 42-103* (this issue), vol. July–September 1990, Jet Propulsion Laboratory, Pasadena, California, pp. 61–69, November 15, 1990.

**Table 1. DSN station Earth orientation partial derivatives<sup>a</sup>**

Station	$\partial r/\partial X$ , cm/cm	$\partial r/\partial Y$ , cm/cm	$\partial z/\partial X$ , cm/cm	$\partial z/\partial Y$ , cm/cm	$\partial \lambda/\partial X$ , nrad/msec	$\partial \lambda/\partial Y$ , nrad/msec
DSS 14	0.2616	-0.5159	-0.3703	0.7301	-0.9914	-0.5027
DSS 43	-0.4954	-0.2979	-0.7018	-0.4220	-0.5723	0.9518
DSS 63	-0.6456	-0.0480	0.7628	0.0567	-0.0986	1.3277

<sup>a</sup> $\partial \lambda/\partial UT = 72.92$  nrad/msec for all stations;  $\partial r/\partial UT, \partial z/\partial UT = 0$  for all stations.

**Table 2. DSN baseline Earth orientation partial derivatives<sup>a</sup>**

Baseline	$\partial r_B/\partial X$ , cm/cm	$\partial r_B/\partial Y$ , cm/cm	$\partial z_B/\partial X$ , cm/cm	$\partial z_B/\partial Y$ , cm/cm	$\partial \lambda_B/\partial X$ , nrad/cm	$\partial \lambda_B/\partial Y$ , nrad/cm
DSS 43-14	-0.3198	-1.1115	0.3315	1.1521	-1.4584	0.4196
DSS 63-14	-0.592	0.0352	-1.1331	0.6735	0.0420	0.0707

<sup>a</sup> $\partial \lambda_B/\partial UT = 72.92$  nrad/msec for all baselines;  $\partial r_B/\partial UT, \partial z_B/\partial UT = 0$  for all baselines.

**Table 3. DSN station location uncertainties**

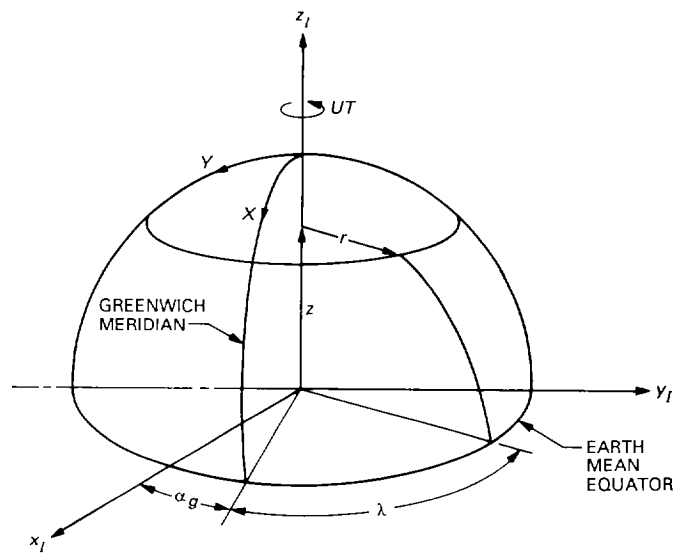
Station	$\sigma_r$ , cm	$\sigma_z$ , cm	$\sigma_\lambda$ , nrad
DSS 14	5.78	8.19	38.1
DSS 43	5.78	8.19	38.1
DSS 63	6.47	7.65	38.8

**Table 4. DSN baseline coordinate uncertainties**

Baseline	$\sigma_{r_B}$ , cm	$\sigma_{z_B}$ , cm	$\sigma_{\lambda_B}$ , nrad
DSS 43-14	11.6	12.0	39.5
DSS 63-14	0.7	13.2	36.5

**Table 5. DSN station and baseline coordinates**

Station	Location	$r_s$ , km	$z_s$ , km	$\lambda$ , deg
DSS 14	Goldstone	5203.997	3677.052	243.1105
DSS 43	Canberra	5205.251	-3674.749	148.9813
DSS 63	Madrid	4862.451	4115.109	355.7520
Baseline	Length (km)	$r_B$ , km	$z_B$ , km	$\lambda_B$ , deg
DSS 43-14	10,588.966	7620.841	7351.801	286.0523
DSS 63-14	8390.430	8378.986	-438.057	210.7265



$(x, y, z)_I$  IS AN EARTH-CENTERED INERTIAL REFERENCE FRAME

Fig. 1. Earth-centered body-fixed and inertial reference frames.